Wiley Online Library
Early View publication on www.wileyonlinelibrary.com
(issue and page numbers not yet assigned;
citable using Digital Object Identifier – **DOI**)

Phys. Status Solidi B, 1–5 (2014) / **DOI** 10.1002/pssb.201451162

physica status solidi b
www.pss-b.com
basic solid state physics

Comparison of carbon nanotube forest growth using AlSi, TiSiN, and TiN as conductive catalyst supports

Junwei Yang[1], Santiago Esconjauregui[*,1], Hisashi Sugime[1], Taron Makaryan[1,2], Toby Hallam[3], Georg S. Duesberg[3], and John Robertson[1]

[1] Department of Engineering, University of Cambridge, CB3 0FA, Cambridge, UK
[2] Faculty of Radiophysics, Yerevan State University, Yerevan 0005, Armenia
[3] Trinity College Dublin, College Green, Dublin 2, ROI, Ireland

Received 15 April 2014, revised 25 June 2014, accepted 7 August 2014
Published online 4 September 2014

Keywords bulk diffusion, carbon nanotubes, conductive supports, forest growth

[*] Corresponding author: e-mail cse28@cam.ac.uk, Phone: +44 1223 748343, Fax: +44 1223 748342

We evaluate carbon nanotube growth by employing AlSi, TiSiN and TiN as conductive catalyst supports. Using a wide range of chemical vapour deposition conditions, we find that only AlSi and TiSiN yield homogeneously-sized nanoparticles, which are stable throughout both catalyst preparation and nanotube synthesis processes. This favours the growth of forests with area densities of the order of 10^{12} nanotubes cm^{-2}. TiN, in contrast, yield lower density forests in a very narrow window process. The forests and the three screened catalyst supports show ohmic conductivity. TiSiN, however, is the only conductor that leads to the very robust growth process. This suggests TiSiN is useful for applications requiring forest growth on conductors and thus warrants further assessment for reducing nanotube diameter and improving area density of the forests.

1 Introduction Owing to their exceptional properties, carbon nanotubes (CNTs) hold many potential applications in various technologies [1–10]. Examples include interconnects in microelectronics, thermal management surfaces, supercapacitors, energy storage, sensors and composites. This has generated a great interest in researching the growth of CNTs, especially on how to control the synthesis of nanotube forests on surfaces [11–15]. The most studied synthesis technique is chemical vapour deposition (CVD). Partly, because CVD is the only growth method that ensures scalability and controllability of nanotube properties.

Each of the envisaged applications of nanotubes demands specific requirements and properties [7–10]. Such as nanotube-based interconnects in microelectronics or heat sinks, which require the tubes in the form of vertically-aligned forests and in direct contact with conductive materials. This is to provide an electrically conductive path through the nanotube support [7, 10]. Herein we concentrate on surface growth CNT CVD aiming to control and to further understand the synthesis of forests directly on a range of conductive supports.

Traditionally, nanotube forests are grown using metal catalysts deposited onto oxide supports. Typical catalyst materials include Ni, Co, Fe, and a combination of them, while oxide supports include mainly Al_2O_3 and SiO_2. The selection of these catalyst supports is related to the surface properties of metals. As oxides have lower surface energies than metals, thin metallic films – deposited onto Al_2O_3 or SiO_2 – easily restructure into nanoparticles during catalyst pretreatment. During catalyst pretreatment, usually by annealing in a reducing atmosphere, the as-formed nanoparticles also undergo reduction. This is an essential step as the particles are catalytically active only in their purely metallic state. The combination of Fe catalyst and Al_2O_3 support has proved the best catalyst system to grow forests. This is because during pretreatment, Fe and Al_2O_3 react at their interface [16]. In reacting, oxygen bridges Fe and Al so that restructuring results in small, homogeneously-sized catalyst nanoparticles. The bridging is so strong that the particles tend to remain immobilised during the whole process of nanotube growth, thus leading to dense nanotube forests. However, the usage of oxides like Al_2O_3 as catalyst supports, especially if the films are continuous or thicker than ~3 nm, is detrimental to the overall conductivity of nanotube forests and support underlayer [17], and ultimately, unsuitable for use as interconnects or heat sinks.

On the other hand, the growth of forests on conductors is very challenging [18–22]. As metals and metal compounds are high-surface-energy materials, it is much more difficult to form and stabilise metallic nanoparticles for nanotube growth. The difficulty stems from the tendency of metals to alloy and inter-diffuse at typical CNT CVD conditions. Also, the support can react with the processing gases degrading its conductive properties. We and others have investigated a number of alternative routes to grow CNT forests directly on metals and/or metal compounds [23–28]. These routes include use of plasma pretreatment prior to CNT CVD [15, 23, 24], use of Co-Mo co-catalyst [25], oxidation of the topmost surface of the support [26], usage of metal silicides as catalyst support [26, 27], employing of a sandwich-like metal stack [28], or enlarging of the grain size of the support material [26]. It is thus possible to grow nanotube forests directly on conductors such as Ti, W, Ta, Cu, TiN or silicides. Nevertheless, nanotube CVD on these materials still remains less robust than on Al_2O_3. The process window is, in general, very narrow and the growth easily leads to poor or lateral growth, rather than nanotube vertical alignment. We therefore need further exploring of materials and processing conditions to benchmark new results against the Al_2O_3/Fe system and so to achieve ultra-high area density forests of (ideally single-walled) CNTs on conductors. The ultimate goal of studying catalyst systems for forest growth is to restructure thin metallic films into catalytically active, homogeneously-sized nanoparticles and immobilise them throughout the whole process of nanotube growth [13].

Herein we compare catalyst formation and nanotube growth on three conductive supports: AlSi, TiSiN and TiN. It is of interest for microelectronics to choose materials which are compatible with its manufacturing processing and thus liable of eventual integration. The three chosen materials are currently used, at some stage, in the production of devices, so that it is worth exploring and comparing their efficiency as catalyst support for nanotube growth. We select AlSi as metal silicides have low surface energies and have proved to yield nanotube forests [26, 27], TiSiN as it is an efficient metal barrier [29, 30], and TiN as it can yield large diameter nanotube forests under certain conditions [26]. From the three materials, TiN is the catalyst support most widely studied in CNT CVD. The growth results on TiN vary dramatically depending on the TiN preparation method, so they are useful for comparison to AlSi and TiSiN. Our results show that, under certain processing conditions, it is possible to grow forests on three the materials. However, the nanotube diameter, area density of the forests and process window are different in all cases. Only AlSi and TiSiN favour the growth of stable, small-diameter nanotubes; TiN yields large-diameter forests at maximum 700 °C; very small size nanoparticles are stable only on TiSiN which also yields the densest forests. Altogether, this screening and comparison of materials allows us to select the most promising candidate for further studying of processing conditions.

2 Experimental details We use as substrate Si coated with 200 nm of thermal SiO_2, on which we deposit (1) 50 nm AlSi formed by direct reaction between 25 nm of poly-crystalline Si and 25 nm of sputtered Al, (2) 50 nm TiSiN by sputtering and (3) 50 nm of TiN by sputtering. Further details of silicidation and conditions for sputtering can be found elsewhere [26]. All samples are exposed to ambient, so could be coated with a native oxide. For catalyst preparation, we evaporate simultaneously on the three supports nominally 0.5, 1.0 or 5.0 nm of high-purity Fe.

For CNT growth, the samples are pretreated in a hot wall CVD system (quartz furnace tube) at 600 to 800 °C in 1 bar Ar:H_2 (1000:500 sccm) for 5 min. The samples are introduced at room temperature (RT) and heated at a nominal heating rate of 100 °C min^{-1}. Immediately after reaching the growth temperature, we introduce C_2H_2 (10 sccm) to the Ar:H_2 flow for 15 min. After growth, the samples are cooled down in a 1000 sccm Ar flow until reaching RT.

The morphology of the catalyst samples is characterised by atomic force microscopy (AFM) and time-of-flight secondary ion mass spectroscopy (TOF SIMS). CNTs are characterised by scanning electron microscopy (SEM) and transmission electron microscopy. The density and size of the nanoparticles are estimated from AFM images using imaging processing software. The densities of the forests are obtained using the weight gain method. Electrical characterisation is performed in a two-terminal Cascade probe station set with a low bias condition ($|V| < 0.05$ V) during all measurements (as to avoid heating effects). The total resistance of the samples is determined from the slopes of a least squares fit to *I*–*V* response. For these measurements, we partially mask the samples during catalyst deposition so that each sample has an area uncovered of forests.

3 Growth and electrical results Figure 1 summarises the growth results for the three conductive supports evaluated here, (a) AlSi, (b) TiSiN and (c) TiN. For a direct comparison, all samples are subject to the same pretreatment and growth conditions. SEM inspections show that, at 700 °C, the three supports yield forests. On AlSi, Fig. 1(a), we obtain an area density of $\sim 10^{11}$ CNTs cm^{-2}. In general, the forests are homogeneous over the samples. The inset in Fig. 1(a) shows the tubes consist of mainly 3–4 walls, with diameters averaging 6 nm. TiSiN also yields high-density forests, Fig. 1(b). The tubes are better aligned than on AlSi. The area density is as high as $\sim 10^{12}$ CNTs cm^{-2}. The inset in Fig. 1(b) indicates that the tubes are slightly smaller, and consist of 2–4 walls, with diameters of ~5 nm. On both supports we employ 1 nm Fe as catalyst. The growth on TiN is rather poor when using such thin films (not shown here), but it yields forests when the Fe thickness is 5 nm, Fig. 1(c). The tubes appear aligned and the area density is lower than on AlSi or TiSiN, of the order of $\sim 10^{10}$ CNTs cm^{-2}. Inset in Fig. 1(c), shows the tubes are multi-walled with diameters ranging between ~6 and 9 nm.

In order to verify whether the forests produced on the screened materials are potentially useful for applications in

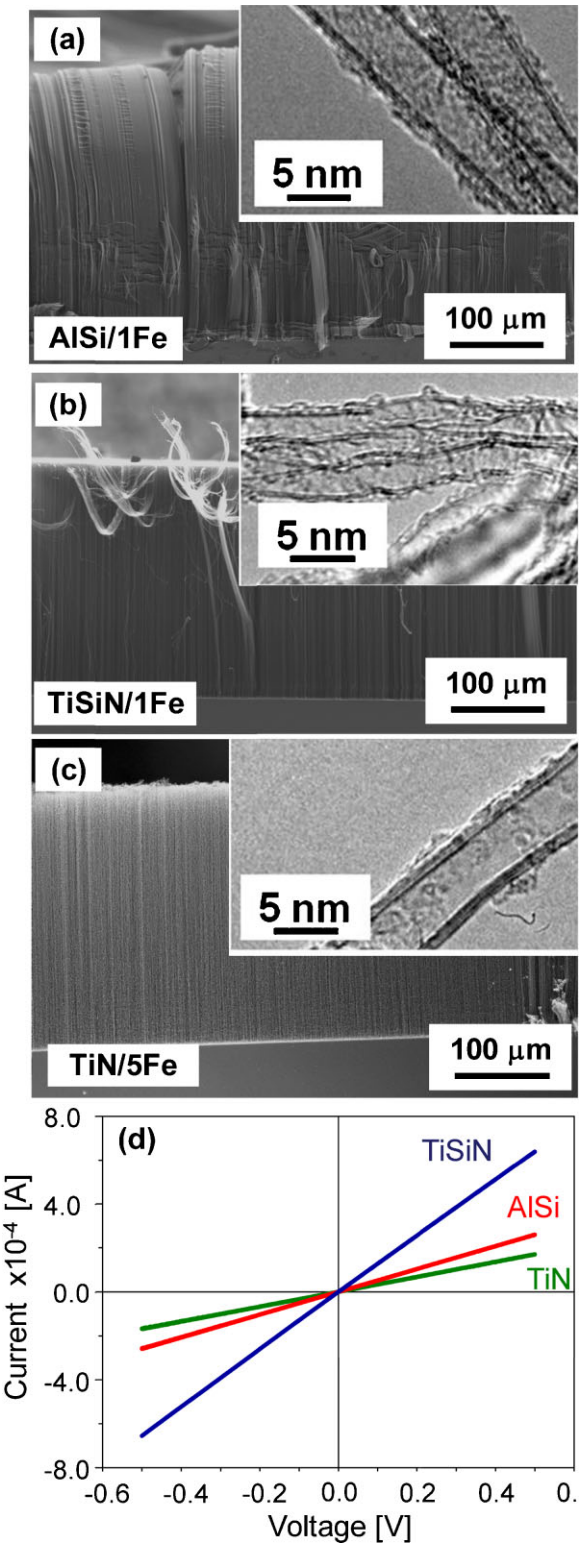

Figure 1 (a)–(c) CNT growth at 700 °C using AlSi, TiSiN and TiN, respectively, as catalyst supports. (d) *I–V* curves obtained on these forests.

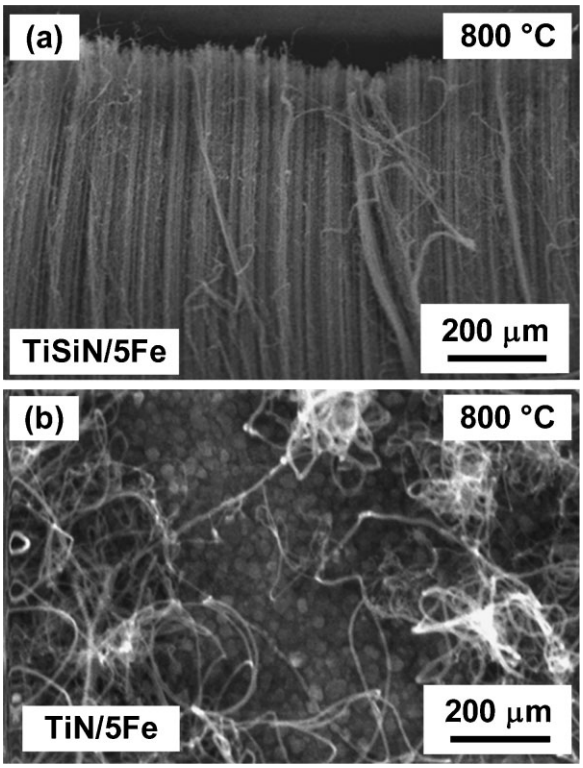

Figure 2 CNT growth at 800 °C using (a) TiSiN and (b) TiN catalyst supports. The poor growth on (b) suggests a strong diffusion of Fe.

microelectronics, we carry out in air current–voltage measurements using a two terminal probe station. Figure 1 (d) shows the *I–V* curves for forests grown at 700 °C. In all cases, we observe Ohmic behaviour. The resistance values are 2.6, 0.8 and 3.4 kΩ for AlSi, TiSiN and TiN respectively. These values compare to previous measurements in the group using similar set up [15]. For a reduction of overall resistance further improvements are still necessary, e.g. by increasing the area density of the tubes, reducing the nanotube diameter, or contacting more walls per unit area. We are currently dealing with CNT CVD on TiSiN, as it shows the most promising figures in terms of nanotube diameter, area density, and electrical response.

We then compare the growth at 800 °C, using 5 nm of Fe catalyst. We select such a thick film as 1 nm Fe yields no growth on TiN. We observe very different growth results, for instance when comparing TiSiN and TiN, Fig. 2. While TiSiN still yields dense forests, Fig. 2(a), TiN shows very poor growth with defective, unaligned tubes, Fig. 2(b). The tube density is very low. This indicates lower catalyst efficiency and suggests Fe diffusion into the TiN underneath, even with increasing the temperature by just 100 °C.

4 Nanoparticle formation The catalyst topography and stability throughout the catalyst formation and growth processes impacts dramatically on the nucleation, growth and morphology of the resulting CNTs. We observe the

formation of high density nanoparticles in temperatures ranging between 600 and 700 °C. AlSi and TiSiN samples yield high-density, homogeneously-sized nanoparticles, as shown in Fig. 3(a) and (b). SEM analysis shows that AlSi presents a nanoparticle lateral size distribution of 7.2 ± 0.4 nm and a nanoparticle number density of $(1.3 \pm 0.6) \times 10^{11}$ cm^{-2}, whereas TiSiN presents a nanoparticle lateral size distribution of 6.6 ± 0.3 nm and a nanoparticle number density of $(1.4 \pm 0.4) \times 10^{11}$ cm^{-2}. This compares to TiN. For 5 nm Fe and same pretreatment conditions, TiN yields particles of $9.3 + 1.1$ nm and a nanoparticle number density of about $(6.1 \pm 0.7) \times 10^{10}$ cm^{-2} (not shown here).

At 800 °C, the restructuring of Fe into nanoparticles depends very much on the type of support. We compare the restructuring of 5 nm Fe. While AlSi and TiSiN show minimal changes on nanoparticle size or density, TiN shows much lower number densities and various size particles. Fe diffusion into the bulk of TiN appears to be more very evident, Fig. 4(a). Conversely on TiSiN, the particles are homogeneous and appear to be much denser, Fig. 4(b). This suggests a strong Fe diffusion into the bulk of TiN, but not into TiSiN.

By TOF-SIMS on both of samples after annealing, we confirm a negligible Fe diffusion into the TiSiN bulk, but a dramatic diffusion of Fe into TiN (not shown here). This is in agreement with previous results on this material [26]. SIMS results prove that TiSiN effectively acts as a diffusion barrier against catalyst diffusion and in a wide range of processing conditions. A complete study will be reported elsewhere.

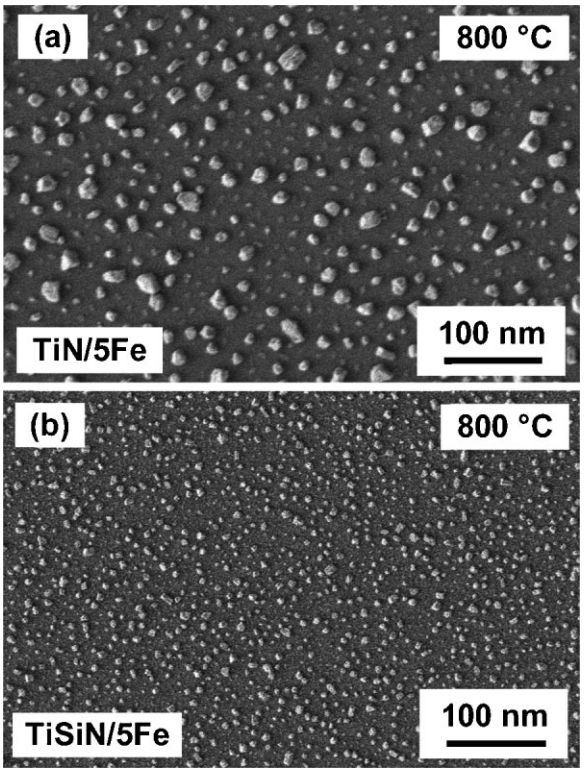

Figure 4 Comparison of nanoparticle formation at 800 °C using 5 nm of Fe deposited onto (a) TiN and (b) TiSiN, respectively.

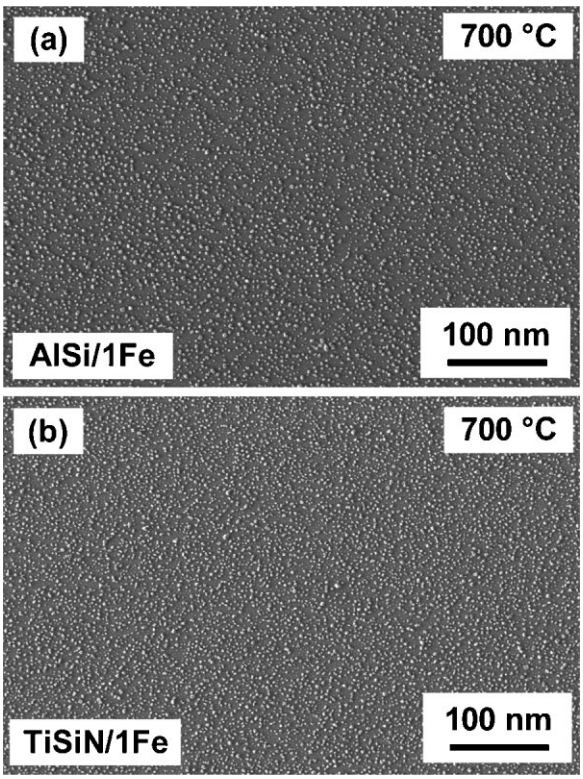

Figure 3 Restructuring of 1 nm Fe into nanoparticles at 700 °C using (a) AlSi and (b) TiSiN, respectively, as catalyst supports.

5 Conclusions In summary we have studied the growth of CNTs on AlSi, TiSiN and TiN conductive catalyst supports. We have found that only AlSi and TiSiN yield small-size nanoparticles which are stable throughout catalyst preparation and nanotube synthesis. This favours the growth of nanotubes forests with area densities of the order of 10^{12} CNT cm^{-2}. These results compare to the growth on TiN which also yields forests, but in a very narrow window process. The forests and the three-screened supports show ohmic conductivity. Since TiSiN leads to the most robust growth process, we suggest it might be useful for applications requiring forest growth on conductors. We are further assessing more catalyst systems and processing conditions aiming to reduce nanotube diameter and thus to improve the area density of the forests on TiSiN and the overall electrical response.

Acknowledgements The authors acknowledge funding from the European projects Technotubes and Grafol.

References

[1] S. S. Fan, M. G. Chapline, N. R. Franklin, T. W. Tombler, A. M. Cassell, and H. J. Dai, Science **283**, 512 (1999).
[2] Q. Ngo, B. A. Cruden, A. M. Cassell, G. Sims, M. Meyyappan, J. Li, and C. Y. Yang, Nano Lett. **4**, 2403 (2004).

[3] M. Nihei, A. Kawabata, D. Kondo, M. Horibe, S. Sato, and Y. Awano, Jpn. J. Appl. Phys., Part 1 **44**, 1626 (2005).
[4] H. Huang, C. H. Liu, Y. Wu, and S. S. Fan, Adv. Mater. **17**, 1652 (2005).
[5] D. N. Futaba, K. Hata, T. Yamada, T. Hiraoka, Y. Hayamizu, Y. Kakudate, O. Tanaike, H. Hatori, M. Yumura, and S. Iijima, Nature Mater. **5**, 987 (2006).
[6] Y. Hayamizu, T. Yamada, K. Mizuno, R. C. Davis, D. N. Futaba, M. Yumura, and K. Hata, Nature Nanotechnol. **3**, 289 (2008).
[7] J. Robertson, G. Zhong, S. Hofmann, B. C. Bayer, C. S. Esconjauregui, H. Telg, and C. Thomsen, Diam. Relat. Mater. **18**, 957 (2009).
[8] D. Acquaviva, A. Arun, S. Esconjauregui, D. Bouvet, J. Robertson, R. Smajda, A. Magrez, L. Forro, and A. M. Ionescu, Appl. Phys. Lett. **97**, 233508 (2010).
[9] Y. Awano, S. Sato, M. Nihei, T. Sakai, Y. Ohno, and T. Mizutani, Proc. IEEE **98**, (2015). (2010
[10] J. Robertson, G. Zhong, S. Esconjauregui, B. Bayer, C. Zhang, M. Fouquet, and S. Hofmann, Jpn. J. Appl. Phys., Part 1 **51**, 01AH01 (002012).
[11] K. Hata, D. N. Futaba, K. Mizuno, T. Namai, M. Yumura, and S. Iijima, Science **306**, 1362 (2004).
[12] K. Hasegawa and S. Noda, ACS Nano **5**, 975 (2011).
[13] S. Esconjauregui, M. Fouquet, B. C. Bayer, S. Eslava, S. Khachadorian, S. Hofmann, and J. Robertson, J. Appl. Phys. **109**, 044303 (2011).
[14] S. Sakurai, H. Nishino, D. N. Futaba, S. Yasuda, T. Yamada, A. Maigne, Y. Matsuo, E. Nakamura, M. Yumura, and K. Hata, J. Am. Chem. Soc. **134**, 2148 (2012).
[15] S. Esconjauregui, B. C. Bayer, M. Fouquet, C. T. Wirth, F. Yan, R. Xie, C. Ducati, C. Baehtz, C. Castellarin-Cudia, S. Bhardwaj, C. Cepek, S. Hofmann, and J. Robertson, J. Appl. Phys. **109**, 114312 (2011).
[16] C. Mattevi, T. Wirth, S. Hofmann, R. Blume, M. Cantoro, C. Ducati, C. Cepek, A. Knop-Gericke, S. Milne, C. Castellarin-Cudia, S. Dolafi, A. Goldoni, R. Schloegl, and J. Robertson, J. Phys. Chem. C **112**, 12207 (2008).
[17] S. Esconjauregui, R. Xie, Y. Guo, S. Pfaendler, M. Fouquet, R. Gillen, C. Cepek, C. Castellarin-Cudia, S. Eslava, and J. Robertson, Appl. Phys. Lett. **102**, 113109 (2013).
[18] T. de los Arcos, F. Vonau, M. G. Garnier, V. Thommen, H.-G. Boyen, P. Oelhafen, M. Dueggelin, D. Mathis, and R. Gugenheim, Appl. Phys. Lett. **80**, 2383 (2002).
[19] Y. Wang, B. Li, P. S. Ho, Z. Yao, and L. Shi, Appl. Phys. Lett. **89**, 183113 (2006).
[20] Y. Wang, Z. Luo, B. Li, P. S. Ho, Z. Yao, L. Shi, E. N. Bryan, and R. J. Nemanich, J. Appl. Phys. **101**, 124310 (2007).
[21] A. M. Rao, D. Jacques, R. C. Haddon, W. Zhu, C. Bower, and S. Jin, Appl. Phys. Lett. **76**, 3813 (2000).
[22] D. Yokoyama, T. Iwasaki, T. Yoshida, H. Kawarada, S. Sato, T. Hyakushima, M. Nihei, and Y. Awano, Appl. Phys. Lett. **91**, 263101 (2007).
[23] S. Esconjauregui, B. Bayer, M. Fouquet, C. Wirth, C. Ducati, S. Hofmann, and J. Robertson, Appl. Phys. Lett. **95**, 173115 (2009).
[24] S. Esconjauregui, C. Cepek, M. Fouquet, B. C. Bayer, A. D. Gamalski, Chen. Bingan, Xie. Rongsi, S. Bhardwaj, C. Ducati, S. Hofmann, and J. Robertson, J. Appl. Phys. **112**, 034303 (2012).
[25] H. Sugime, S. Esconjauregui, J. Yang, L. D'Arsié, R. Oliver, S. Bhardwaj, C. Cepek, and J. Robertson, Appl. Phys. Lett. **103**, 109901 (2013).
[26] S. Esconjauregui, S. Bhardwaj, J. Yang, C. Castellarin-Cudia, R. Xie, L. D'Arsié, T. Makaryan, H. Sugime, S. Fernandez, C. Cepek, and J. Robertson, Carbon **73**, 13 (2014).
[27] C. Zhang, F. Yan, C. S. Allen, B. C. Bayer, S. Hofmann, B. J. Hickey, D. Cott, G. Zhong, and J. Robertson, J. Appl. Phys. **108**, 24311 (2010).
[28] G. Zhong, R. Xie, J. Yang, and J. Robertson, Carbon **67**, 680 (2014).
[29] M. S. Angyal, Y. Shacham-Diamand, J. S. Reid, and M.-A. Nicolet, Appl. Phys. Lett. **67**, 2152 (1995).
[30] J. K. Schaeffer, S. B. Samavedam, D. C. Gilmer, V. Dhandapani, P. J. Tobin, J. Mogab, B.-Y. Nguyen, B. E. White, J. S. Dakshina-Murthy, R. S. Rai, Z.-X. Jiang, R. Martin, M. V. Raymond, M. Zavala, L. B. La, J. A. Smith, R. Garcia, D. Roan, M. Kottke, and R. B. Gregory, J. Vac. Sci. Technol. B **21**, 11 (2003).